

ON THE GENERALIZED KRAMERS PROBLEM WITH EXPONENTIAL MEMORY FRICTION*

Katja Lindenberg[†]

Department of Chemistry and Biochemistry 0340
and Institute for Nonlinear Science
University of California San Diego
La Jolla, California 92093-0340

Aldo H. Romero

Department of Chemistry and Biochemistry 0340
and Department of Physics
University of California, San Diego
La Jolla, California 92093-0340

José M. Sancho

Institute for Nonlinear Science 0402
University of California San Diego
La Jolla, California 92093-0402

and

Departament d'Estructura i Constituents de la Matèria
Universitat de Barcelona

August 4, 2018

Abstract

The time-dependent transmission coefficient for the generalized Kramers problem with exponential memory friction has recently been calculated by Kohen and Tannor [D. Kohen and D. J. Tannor, *J. Chem. Phys.* **103**, 6013 (1995)] using a procedure based on the method of reactive flux and the phase space distribution function. Their analysis is restricted to the high friction regime or diffusion-limited regime. We recently developed a complementary theory for the low-friction energy-diffusion-limited regime in the Markovian limit [Sancho et al., to appear in *J. Chem. Phys.*; cond-mat/9806001]. Here we generalize our method to the case of an exponential dissipative memory kernel. We test our results, as well as those of Kohen and Tannor, against numerical simulations.

*Abbreviated Running Title: ON THE GENERALIZED KRAMERS PROBLEM

[†]Corresponding author. Department of Chemistry and Biochemistry 0340, UCSD, 9500 Gilman Dr., La Jolla, CA 92093-0340. Phone: (619) 534-3285. FAX: (619) 534-7244. Email: klindenberg@ucsd.edu

Key Words: Kramers, Transmission Coefficient, Energy-limited, Exponential Memory

PACS Codes: 05.20.-y, 10.40.+j

1 Introduction

The classic work of Kramers [1] on reaction rates in which the effect of the solvent was taken into account in the form of a Markovian dissipation and Gaussian delta-correlated fluctuations has spawned an enormous and important literature that continues to flourish [2, 3, 4, 5]). The enormous literature on the theoretical front since the appearance of Kramers' seminal paper has evolved in many directions that include more formal derivations of Kramers' own results, extensions to larger parameter regimes and to non-Markovian dissipation models, generalizations to more complex potentials and to many degrees of freedom, analysis of quantum effects, and application to specific experimental systems.

One recent direction, developed by Kohen and Tannor (KT) [6], deals with the derivation of the rate coefficient in the Kramers problem and in the more general Grote-Hynes problem [7] (that is, the Kramers problem extended to a non-Markovian dissipative memory kernel) so as to obtain not only the asymptotic rate constant but the behavior of the rate coefficient at all times. This derivation is based on the reactive flux method [2, 8, 9], thus paralleling closely and usefully the methods used in numerical simulations of the problem. KT analyze in detail the time it takes the rate coefficient to reach its stationary (equilibrium) value and the way in which this value is approached. Their extensive analysis, however, does not cover a number of parameter regimes, nor do they check their time-dependent results against numerical simulations. In this paper we complement their work by extending the parameter regime of analysis and checking their results as well as our new ones against numerical simulations.

The non-Markovian generalization of the Kramers problem is based on the dynamical equations [7]

$$\begin{aligned}\dot{q} &= \frac{p}{m} \\ \dot{p} &= - \int_0^t dt' \Gamma(t-t') p(t') - \frac{dV(q)}{dq} + f(t)\end{aligned}\tag{1}$$

where $q(t)$ is the time-dependent reaction coordinate, a dot denotes a time derivative, $\Gamma(t-t')$ is the

dissipative memory kernel, $V(q)$ is the potential energy, and $f(t)$ represents Gaussian fluctuations that satisfy the fluctuation-dissipation relation

$$\langle f(t)f(t') \rangle = k_B T \Gamma(t - t'). \quad (2)$$

k_B is Boltzmann's constant and T is the temperature. The potential $V(q)$ is a double-well potential that is often (and here as well) taken to be of the form

$$V(q) = V_0 \left(\frac{q^4}{4} - \frac{q^2}{2} + \frac{1}{4} \right) = \frac{V_0}{4} (q^2 - 1)^2. \quad (3)$$

The parameter V_0 can be used as the unit of energy, and henceforth we set it equal to unity. The barrier height is assumed to be large compared to the temperature (i.e., $k_B T \ll 1/4$).

The problem of interest is the time-dependent rate coefficient $k(t)$ for an ensemble of particles whose positions evolve as realizations of $q(t)$. The coefficient $k(t)$ measures the mean rate of passage of the ensemble across the barrier at $q = 0$ from one well to the other. The asymptotic value of this crossing rate, $k \equiv k(\infty)$, is associated with the rate constant of the process represented by the reaction coordinate. One usually focuses on the corrections to the rate obtained from transition state theory (TST) and therefore writes

$$k(t) = \kappa(t) k^{TST} \quad (4)$$

where k^{TST} is the rate obtained from transition state theory for activated crossing, which for our problem and in our units is [2, 3, 10]

$$k^{TST} = \frac{\sqrt{2}}{\pi} e^{-1/4k_B T}. \quad (5)$$

The deviations from this rate constant are then contained in the transmission coefficient $\kappa(t)$. The construction of $\kappa(t)$ is discussed in subsequent sections.

In this paper, as do KT, we deal with the exponential memory kernel

$$\Gamma(t) = \frac{\gamma}{\tau} e^{-|t|/\tau} \quad (6)$$

where γ is the dissipation parameter and τ is the correlation time. The Kramers problem corresponds to the limit $\tau \rightarrow 0$. In their work, KT derived an expression for $\kappa(t)$ in terms of the

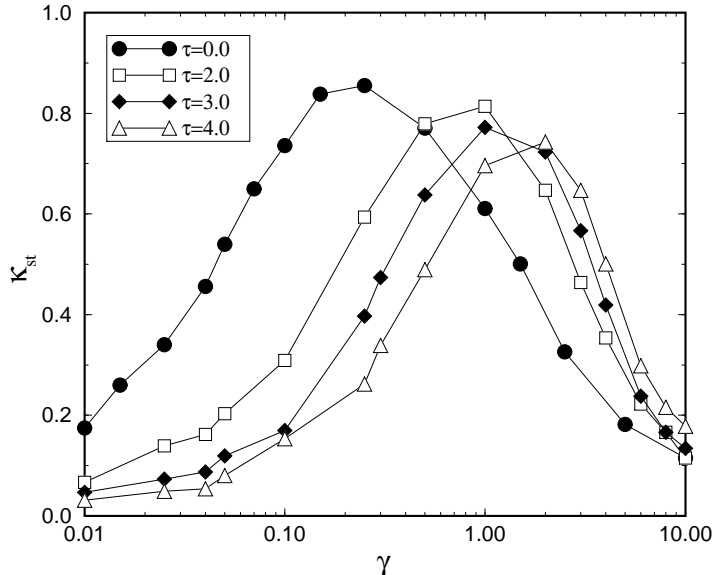


Figure 1: Transmission coefficient κ_{st} vs dissipation parameter γ for $k_B T = 0.025$ and various values of the memory correlation time τ . These results are obtained from direct simulation of Eq. (1) as described in Section 2.2. As is well known, the turnover moves to higher values of the friction parameter with increasing τ because the effective dissipation at given γ is weaker as τ increases. Also, the maximum transmission coefficient decreases with increasing τ .

time-dependent phase space density, assumed a particular form for this density, and studied how $\kappa(t)$ goes to its steady state value as the phase space density relaxes to equilibrium. In carrying out this program, however, they relied on approximations that are appropriate only for the diffusion limited regime (large γ) and therefore were able to calculate $\kappa(t)$ only in this regime.

In a recent paper [10] we developed a theory for the time-dependent transmission coefficient in the energy-diffusion-limited regime (small γ) for the original Kramers model. Thus, to supplement the work of KT and our own work in the Markovian regime, here we formulate the complementary theory for the time-dependent transmission coefficient in the non-Markovian energy-diffusion-limited regime and compare our results with numerical simulations in this regime. As in the Markovian case [10], our theory captures the complex oscillatory and stationary state behavior of $\kappa(t)$ in this regime very well. We also carry out simulations of the time-dependent transmission coefficient in the diffusion-limited regime to assess and confirm the validity of the KT formulation. We will show examples of the good agreement of their results with simulations, both in the

“non-adiabatic” regime (large γ but $\gamma < \tau$) and in the “caging” regime (large γ with $\gamma > \tau$).

In Section 2 we briefly review the reactive flux formalism and describe the numerical methods used in our simulations to implement the formalism. Typical simulation results in various regimes are shown in this section. In Section 3 we recall the theoretical methods of analytic calculation of the transmission coefficient in the diffusion-limited regime (that is, KT’s method) and energy-diffusion-limited regime (our method). The generalization of our previous Markovian results to the non-Markovian regime is detailed in this section, as are comparisons of these various results with numerical simulations. We conclude in Section 4.

2 Reactive Flux Formalism and Simulations

2.1 Reactive Flux Formalism

Two decades ago saw the development of the reactive flux formalism for the rate constant over a barrier [2, 8, 9]. This formalism was important because it made possible the efficient numerical simulation of rate constants without having to wait the inordinately long time that it takes a particle at the bottom of one well to climb up to the top of the barrier. In the reactive flux method the problem is formulated in terms of the particles of the distribution that are sufficiently energetic to be above the barrier at the outset. In this way, it is not necessary to wait for low-energy particles (the vast majority of all the particles) to first acquire sufficiently high energies via thermal fluctuations.

We follow the notation of KT. The rate constant $k(t)$ in the reactive flux formalism is

$$k(t) = \frac{\langle \dot{\theta}_P(q_0) \theta_P[q(q_0, v_0, t)] \rangle}{\langle \theta_R(q_0) \rangle} = \frac{\langle v_0 \delta(q_0) \theta_P[q(q_0, v_0, t)] \rangle}{\langle \theta_R(q_0) \rangle}, \quad (7)$$

where the top of the barrier is at position $q_0 = 0$, $\theta_R(x) = 1$ if $x < 0$ and 0 otherwise, and $\theta_P = 1 - \theta_R$. The brackets $\langle \rangle$ represent an average over initial equilibrium conditions. With the particular choices made in Eq. (7) one is calculating the transition rate *from* the left well *to* the right. KT proceed through a series of steps that finally yield for the transmission coefficient introduced in Eq. (4) the relation

$$\kappa(t) = \frac{m}{k_B T} \int_{-\infty}^{\infty} dv_0 v_0 e^{-mv_0^2/2k_B T} \chi(v_0, t) \quad (8)$$

where

$$\chi(v_0, t) = \int_0^\infty dq \int_{-\infty}^\infty dv W(q, v, t; q_0 = 0, v_0) \quad (9)$$

and $W(q, v, t; q_0 = 0, v_0)$ is the conditional phase space distribution function that corresponds to an ensemble of particles starting at $(q_0 = 0, v_0)$ at $t = 0$.

The (nonequilibrium) conditional probability distribution W clearly lies at the crux of the calculation: it is the distribution associated with the generalized Langevin equation (1). In Section 3 we discuss the approximate solution of this problem (which can not be solved exactly) to obtain analytic results. The above definitions are sufficient for the numerical simulations.

2.2 Numerical Simulation Method

The numerical solution of Eqs. (1) is performed according to the following main steps. First, we write the problem in the entirely equivalent form[11, 12]

$$\dot{q} = \frac{p}{m}, \quad \dot{p} = -\frac{dV(q)}{dq} + z, \quad \dot{z} = -\gamma \frac{p}{\tau} - \frac{z}{\tau} + \eta(t) \quad (10)$$

where

$$\langle \eta(t)\eta(t') \rangle = \frac{2\gamma k_B T}{\tau^2} \delta(t - t'). \quad (11)$$

The integration of this set of equations is carried out using the second order Heun's algorithm [13], which has been tested in different stochastic problems with very reliable results [14]. A very small time step is used, ranging from 0.001 to 0.0001, as in Ref. [8]. The numerical evaluation of the transmission coefficient $\kappa(t)$ follows the description of Refs. [8, 9]. We start the simulation with N particles (between 1000 and 4000 depending on the circumstances), all of them above the barrier at $q = 0$, half with a positive velocity distributed according to the Boltzmann distribution in energy, which translates to the velocity distribution $v \exp(-v^2/2k_B T)$, and the other half with the same distribution but with negative velocities. The transmission coefficient is extracted from these sets of simulated data by calculating [8]

$$\kappa(t) = \frac{N_+(t)}{N_+(0)} - \frac{N_-(t)}{N_-(0)}, \quad (12)$$

where $N_+(t)$ and $N_-(t)$ are the particles that started with positive velocities and negative velocities respectively and at time t are in or over the right hand well (i.e. the particles for which $q(t) > 0$).

As discussed by Straub et al. [9], whereas the exact transmission coefficient reaches a constant non-zero value that corresponds to the equilibrium transition rate for the problem, the transmission coefficient calculated using the reactive flux method flattens out but continues to decrease with time. If the temperature is low, this decrease is slow and the results appear flat for rather long simulation times. In this case the value of $\kappa(t)$ in this flat region is identified with κ_{st} . If the temperature is not so low, then the decaying tail is extrapolated back to its intersection with the vertical axis according to the relation $\kappa(t) \sim \kappa_{st}e^{-Kt}$ where K is the decay constant of the tail. The value of the intersection is then identified as κ_{st} .

2.3 Simulation Results

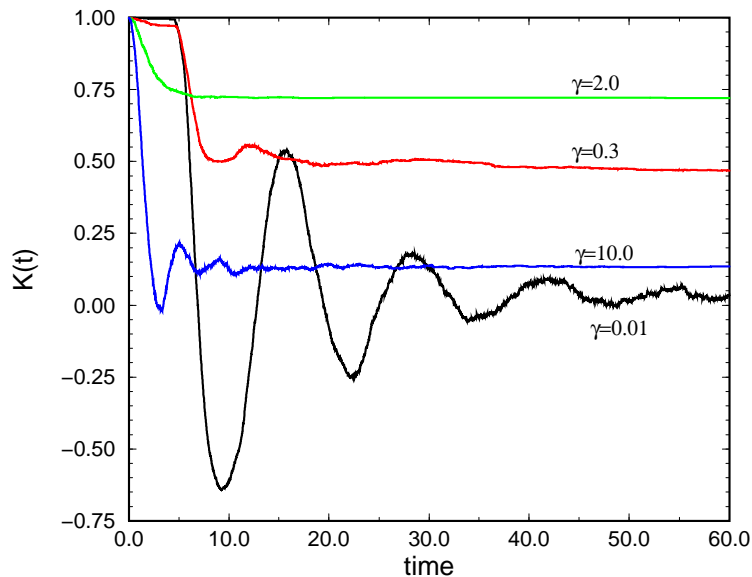


Figure 2: Numerical simulation results for the transmission coefficient $\kappa(t)$ vs time for memory correlation time $\tau = 3.0$ and temperature $k_B T = 0.025$, and four values of the dissipation parameter γ . Diffusion-limited non-adiabatic regime: $\gamma = 2$; diffusion-limited caging regime: $\gamma = 10$; energy-diffusion-limited regime: $\gamma = 0.01$; intermediate regime: $\gamma = 0.3$.

Figure 2 exhibits examples of the temporal behavior of the transmission coefficient, Eq. (12), associated with the system (1), for four typical different parameter regimes. The input parameters

of the problem are the dissipation parameter γ , the correlation time τ , and the temperature $k_B T$. The memory correlation time in the figure is held fixed at the value $\tau = 3.0$ and the temperature at $k_B T = 0.025$. The $\gamma = 2.0$ curve is typical of the diffusion-limited “non-adiabatic” regime. This is beyond the turnover value for $\tau = 3.0$ in Fig. 1 but still small enough to be in the non-adiabatic regime. The transmission coefficient decays monotonically to the equilibrium plateau. The curve differs from the typical behavior in the Markovian diffusion-limited regime [10, 6] in that the initial decay is Gaussian rather than exponential [6] (this detail is just barely visible in the figure). The $\gamma = 10.0$ curve is typical of the regime well beyond the turnover dissipation and well into the “caging regime” [6]. The transmission coefficient decays in an oscillatory fashion with an oscillation frequency that can be associated with an effective potential discussed later. The $\gamma = 0.01$ curve is typical of very low dissipation, well within the energy-diffusion-limited regime. The transmission coefficient remains at its initial value up to a time beyond which it decays in an oscillatory manner to its equilibrium value. As shown later, this behavior is quantitatively captured by our theory. The oscillation frequency in this case is completely different from that of the caging regime. Finally, $\gamma = 0.3$. is below the turnover in Fig. 1 but not much below, and the associated transmission coefficient exhibits a mixture of features characteristic of diffusion-limited behavior (the initial decay to an apparent plateau) and energy-diffusion-limited behavior (the subsequent oscillatory decay to equilibrium).

3 Theory

The conditional probability distribution $W(q, v, t; q_0 = 0, v_0)$ associated with Eq. (1) can not be calculated exactly for the bistable potential (3). Various approximations associated with different parameter regimes and the resulting time-dependent transmission coefficients are discussed in this section.

3.1 Diffusion-Limited Regime

KT focus on the regime of moderate to high dissipation, the regime first discussed in detail by Grote and Hynes [7]. This is the regime to the right of the turnover in Fig. 1; the specific values of γ included in this regime clearly depend on the correlation time τ . To obtain an explicit expression for the probability distribution W , KT adapt the theory of Adelman [15] to the assumption that the barrier is parabolic and the wells are infinitely deep. With this approximation, KT derive

expressions for $\kappa(t)$ from which the Grote-Hynes equilibrium results for the transmission coefficient are recovered in the long-time limit. For arbitrary times they obtain the expression

$$\kappa(t) = \frac{C_v(t)}{\sqrt{C_v^2(t) + \frac{mA_{11}(t)}{k_B T}}} \quad (13)$$

where

$$A_{11}(t) = -\frac{k_B T}{m} (C_v^2(t) - C_q^2(t) + 1), \quad (14)$$

$$C_q(t) = 1 + \int_0^t dt' C_v(t'), \quad (15)$$

and

$$C_v(t) = \mathcal{L}^{-1}[s^2 - 1 + s\hat{\Gamma}(s)]^{-1} = \sum_i c_i e^{\mu_i t}. \quad (16)$$

Here \mathcal{L}^{-1} denotes the inverse Laplace transform, $\hat{\Gamma}(s)$ is the Laplace transform of the memory kernel $\Gamma(t)$, and the μ_i are the roots of $s^2 - 1 + s\hat{\Gamma}(s) = 0$. For the exponential memory kernel (6) $\hat{\Gamma}(s) = \gamma/(1 + \tau s)$; the equation is then cubic so there are three roots μ_i . The largest one of them is positive and it determines the equilibrium transmission coefficient. The others may be real or complex, depending on the parameter values, and this in turn determines whether the transmission coefficient approaches equilibrium in an oscillatory or monotonic fashion. KT show that in the Markovian regime ($\tau \rightarrow 0$) the decay of $\kappa(t)$ is monotonic and exponential. On the other hand, for τ large compared to the time scale μ_1 of the reaction (the precise limits on τ for this to be the case are discussed in KT), they show that in the so-called “non-adiabatic” regime the decay is monotonic, whereas in the “caging” regime the decay is oscillatory. This behavior is easy to understand: for a time interval smaller than τ one can roughly approximate $\Gamma(t - t')$ as constant. Performing the integral in Eq. (1) over such a time interval, one obtains an effective potential V_{eff} of the form

$$V_{eff}(q) = V(q) + \frac{\gamma q^2}{\tau 2}. \quad (17)$$

If $\gamma < \tau$ (non-adiabatic regime), this is still a bistable potential, albeit with a smaller barrier than that of the “bare” potential $V(q)$. However, if $\gamma > \tau$ (caging regime), then the effective potential over this time interval is monostable with a frequency $\omega_{caging} \sim (\gamma/\tau - 1)^{1/2}$ about $q = 0$.

In Fig. 3 we show again two of the simulation results shown in Fig. 2, those for which the KT theory is valid, as well as the results of Eq. (13). The monotonic “non-adiabatic” decay and the oscillatory “caging” decay are clearly captured very well by the theory, including the oscillation frequency in the latter (which for these parameters is $\omega_{caging} = 1.53$) and the equilibrium values in both cases.

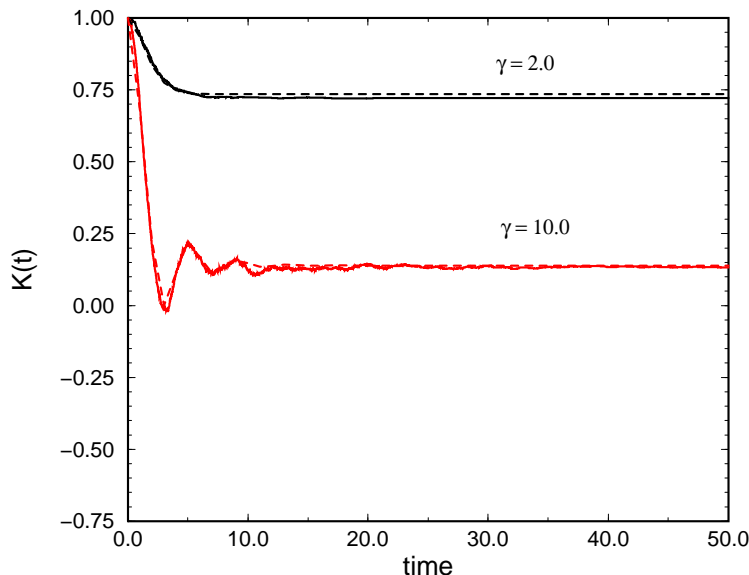


Figure 3: Numerical simulation results and theoretical results for the transmission coefficient $\kappa(t)$ vs time for memory correlation time $\tau = 3.0$ and temperature $k_B T = 0.025$, and two values of the dissipation parameter γ in the diffusion-limited regime. Solid curves: simulation results for $\gamma = 2.0$ (diffusion-limited non-adiabatic regime) and $\gamma = 10.0$ (diffusion-limited caging regime). The dashed curves in each case are calculated from the theory of Kohen and Tannor as given in Eq. (13).

The KT theory is not appropriate for low dissipation parameters and indeed it fails in that regime because it does not take into account the inertial recrossing of the barrier that dominates this regime. Thus, a different approach is required in that case

3.2 Energy-Diffusion-Limited Regime

When the dissipation is very slow, that is, well to the left of the turnover in Fig. 1, the dynamics of the system is dominated by the slow variation of the energy. Thus, a particle that starts above the barrier may recross the barrier many times before it loses sufficient energy to be trapped in one well or the other. We note that there are interesting questions concerning the role and applicability of the reactive flux method and hence of the transmission coefficient in the prediction of time-dependent reaction rates in the low dissipation regime [3]. Here we do not deal with these issues. Rather, we take the reactive flux method as our starting point and carry out our analysis within that framework.

Because of the slow energy variation it is here convenient to rewrite the dynamical equations (1) in terms of the displacement and the *energy* (henceforth we set the mass m equal to unity)

$$E = \frac{p^2}{2} + V(q) \quad (18)$$

instead of the momentum [16, 17]. This simple change of variables leads to

$$\dot{q} = p(t) \quad (19)$$

$$\dot{E} = -p(t) \int_0^t dt' \Gamma(t-t') p(t') + f(t)p(t) \quad (20)$$

where $p(t)$ is understood as a shorthand notation for $\{2[E(t) - V(q(t))]\}^{1/2}$. This set can of course not be solved exactly either, but one can take advantage of the fact that for slow dissipation the temporal variation of the energy is much slower than that of the displacement.

When dissipation is very slow, the particles that start above the barrier lose their energy very slowly as they orbit around at an almost constant energy during each orbit (recrossing the barrier many times if they start with sufficiently high energy). One can calculate the approximate energy loss per orbit and thus keep track of how long it takes a particle of a given initial energy above the barrier to lose enough energy to be trapped in one well or the other. There is a distribution of such particles above the barrier, and the time that it takes the ensemble to lose enough energy to be trapped in a well is correspondingly distributed.

The principal ingredients in the calculation of the transmission coefficient are: 1) The time t_ε that it takes an orbiting particle of energy ε above the barrier to complete a half orbit, that is, to

return to $q = 0$; 2) The energy loss in a half orbit, $\mu(\varepsilon)$, of a particle of initial energy ε above the barrier; and 3) The distribution of times at which particles eventually become trapped in one well or the other.

To calculate the time that it takes a particle of energy ε above the barrier ($E = 1/4 + \varepsilon$) to complete one passage from $q = 0$ to the edge q_+ of the potential well and back to $q = 0$, we assume that the energy remains fixed during this passage. q_+ is given by the solution of $E = V(q)$, i.e., by $q_+ = (1 + \sqrt{4E})^{1/2}$. Independently of the value of τ and γ , the time t_ε for this half-orbit is then simply obtained by integrating Eq. (19):

$$t_\varepsilon = 2 \int_0^{q_+} \frac{dq}{\{2[E - V(q)]\}^{1/2}}. \quad (21)$$

With the potential (3) this can be expressed in terms of a complete elliptic integral of the first kind. For low temperatures the particles that determine the behavior of the transmission coefficient are primarily those just above the top of the barrier. For these energies an excellent approximation to the complete elliptic integral yields[3, 10]

$$t_\varepsilon \approx \ln \frac{16}{(E - \frac{1}{4})} = \ln \frac{16}{\varepsilon}. \quad (22)$$

The corrections to Eq. (22) are of $O(\varepsilon \ln \varepsilon)$.

The energy of the particle of course does not in fact remain constant as the particle orbits around. The calculation of $\mu(\varepsilon)$ will be postponed for the moment – we return to it later in this section. The result does of course depend on γ , τ , and temperature. Suffice it for now to say that to an acceptable level of approximation the energy loss μ can be taken to be independent of ε . Although this assumption is not essential, it does simplify the calculations considerably.

The steps in the construction of the transmission coefficient from these components have been

detailed in our earlier work[10]. Here we simply display and interpret the final result:

$$\begin{aligned}
\kappa(t) &= 1 + 2 \sum_{n=1}^{\infty} (-1)^n e^{-f_n(t)/k_B T}, & 0 < t < \ln \frac{16}{\mu}, \\
&= 1 - 2e^{-\mu/k_B T} + 2 \sum_{n=2}^{\infty} (-1)^n e^{-f_n(t)/k_B T}, & \ln \frac{16}{\mu} < t < 2 \ln \frac{16}{(2!)^{1/2} \mu}, \\
&= 1 - 2e^{-\mu/k_B T} + 2e^{-2\mu/k_B T} + 2 \sum_{n=3}^{\infty} (-1)^n e^{-f_n(t)/k_B T}, & 2 \ln \frac{16}{(2!)^{1/2} \mu} < t < 3 \ln \frac{16}{(3!)^{1/3} \mu},
\end{aligned} \tag{23}$$

and so on. The function $\varepsilon = f_m(t)$ is the solution of the relation $t = t_\varepsilon + t_{\varepsilon-\mu} + \dots + t_{\varepsilon-(m-1)\mu}$, which upon exponentiation turns into the m^{th} order polynomial equation

$$(16)^m e^{-t} = \varepsilon[\varepsilon - \mu] \cdots [\varepsilon - (m-1)\mu]. \tag{24}$$

The solution of Eq. (24) can in general not be found in closed form for $m \geq 3$. However, an excellent approximation is

$$f_m(t) \approx \left[m - (m!)^{1/m} \right] \mu + 16e^{-t/m}. \tag{25}$$

This form is exact for $m = 1$, and it is exactly correct for all m at the upper limit of the time range that defines the trapping of the particles whose initial energy is $\varepsilon = m\mu$. In other words, $f_m(t)$ as given in Eq. (25) is exactly correct at the particular time $t = t_\mu + t_{2\mu} + \dots + t_{m\mu}$. The asymptotic limit of Eq. (23) gives for the equilibrium transmission coefficient

$$\kappa_{st} \equiv \kappa(t \rightarrow \infty) = 1 + 2 \sum_{n=1}^{\infty} (-1)^n e^{-n\mu/k_B T} = \tanh \left(\frac{\mu}{2k_B T} \right). \tag{26}$$

It is useful to examine the information contained in the various contributions to Eq. (23). The first line contains all first recrossings of the barrier by all particles that start with sufficient energy above the barrier to recross is at least once ($\varepsilon > \mu$). The function $f_1(t)$ accounts for the fact that this first recrossing occurs at different times for particles of different initial energy, the last ones (those closest to the barrier that do make it around) recrossing at time $t = \ln(16/\mu)$. The

particles of higher energy recross first because they are orbiting at higher velocity, and may be back for their second recrossing while those of lower energy are still awaiting their first crossing. The time distribution of the second recrossing is contained in $f_2(t)$. Even while this is occurring, some particles might already be undergoing their third recrossing, as contained in $f_3(t)$. There are fewer and fewer of these faster particles because of their initial thermal distribution – this information, too, is contained in the exponential factors. Of course while all these recrossings are going on, the particles are losing energy and, depending on their initial energy and how often they have gone around, they become trapped at sequential times as expressed in the subsequent lines of Eq. (23). In constructing these results we have averaged over a half orbit in calculating the time for the return of a particle to the origin, and have assumed that in the calculation of this period the energy loss of the particle over the half orbit is negligible. Thus, we have approximated the evolution of the energy of a particle as determined by Eqs. (19) and (20) with $f(t) = 0$ by simply assuming an energy loss of μ at the end of each half orbit.

The only remaining calculation is that of the energy loss μ per half orbit. This quantity must be calculated from the generalized Langevin equation Eq. (20).

3.2.1 Markovian limit

In our earlier work [10] we detailed and discussed the calculation of μ for the Markovian case. We showed that when the fluctuations are ignored entirely, the equation for the rate of change of the energy, $\dot{E} = -2\gamma[E - V(q)]$, averaged over a half-orbit leads to the approximate equation

$$\dot{E} \approx -\frac{4\gamma}{3} \frac{1}{t_{E-1/4}}. \quad (27)$$

Integration then directly leads to an implicit algebraic equation for $\mu(\varepsilon)$ [10]. It turns out that μ does depend on the initial energy ε of the particle above the barrier – specifically, μ increases with increasing ε , but that this dependence is mild, as seen in Fig. 4 for two values of the dissipation parameter. An upper bound is the simple relation between the energy loss per half orbit and the dissipation parameter

$$\mu = \frac{4}{3}\gamma. \quad (28)$$

This result agrees with that obtained via weak-collision arguments or small dissipation arguments by a variety of essentially equivalent routes. The total variation of μ with ε is of order 10% for

dissipation parameters in the energy-diffusion limited regime, as can be seen in the figure.

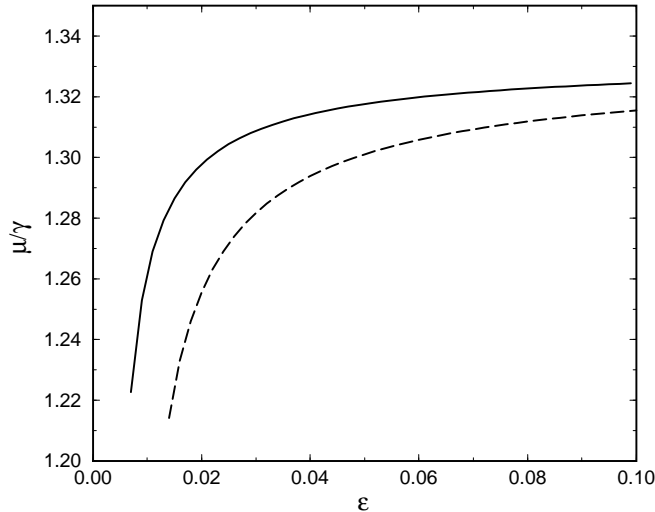


Figure 4: Energy loss per half orbit as a function of energy in the Markovian limit ($\tau \rightarrow 0$) for two values of the dissipation parameter: $\gamma = 0.005$ (dashed curve) and $\gamma = 0.01$ (solid curve).

Thermal effects tend to reduce μ since thermal fluctuations allow the particle to gain some energy as it orbits. We refer the reader to Ref. [10] for a discussion of thermal effects.

Figure 5 shows the transmission coefficient $\kappa(t)$ as a function of time in the Markovian limit ($\tau \rightarrow 0$) for a typical set of parameters in the energy-diffusion-limited regime. The distinctive features of the time dependence are 1) the time at which the transmission coefficient drops rather abruptly from its initial value of unity, and the slope of this drop; 2) the frequencies and amplitudes of the oscillations; and 3) the asymptotic value, identified as the equilibrium value κ_{st} of the transmission coefficient. The dashed curve is the result of our theory, Eq. (23), with the bare value $\mu = 4\gamma/3$ for the energy loss per half orbit. We stress that there are no adjustable parameters in these curves. The agreement between the theory and simulations is clearly very good, and typical of parameters in this regime. Without adjustable parameters, the theory captures each of the three distinctive features listed above. Indeed, we stress that with a single expression we are able to reproduce the temporal behavior of the system over essentially *all* time scales.

The theoretical equilibrium value of the transmission coefficient achieved by the dashed curve in Fig. 5 is a little higher than the simulation result. We also show the equilibrium transmission coefficient obtained when we include thermal effects [10] (thick short line that intersects the right

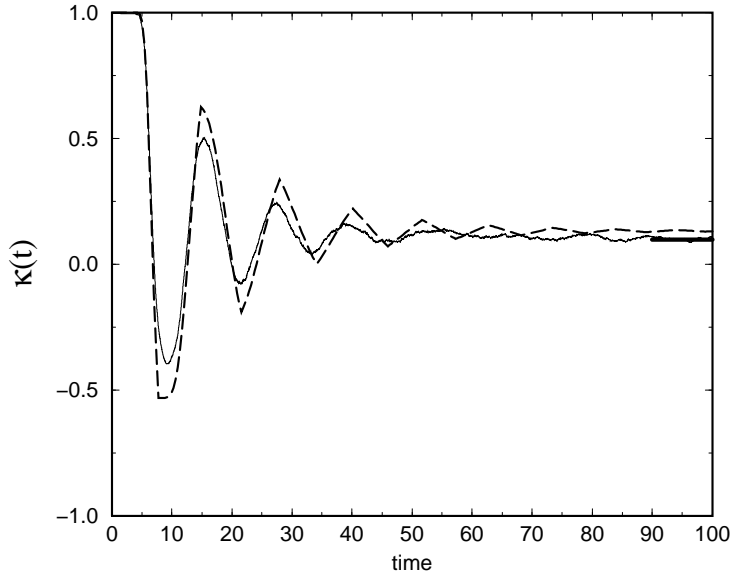


Figure 5: Transmission coefficient of an ensemble of particles at temperature $k_B T = 0.025$ and dissipation parameter $\gamma = 0.005$ in the Markovian limit. Solid curve: simulation of 4000 particles. Dashed curve: our theory, Eq. (23), with the bare value $\mu = 4\gamma/3 = 0.006667$. Thick line that intersects the right vertical axis: value of the equilibrium transmission coefficient κ_{st} obtained from Eq. (26) using the value of μ renormalized by thermal fluctuations, which for this temperature is $\mu(T) = 0.004907$.

vertical axis). This value of the stationary transmission coefficient agrees extremely with the simulation result. In [10] we discuss the connection of our equilibrium result to other predictions [18].

3.2.2 Non-Markovian limit

To calculate μ in this regime we again begin by ignoring the fluctuations and thus approximate the energy evolution by the first portion of Eq. (20),

$$\dot{E} = -p(t) \int_0^t dt' \Gamma(t-t') p(t'), \quad (29)$$

where $p(t) \equiv \{2[E(t) - V(q(t))]\}^{1/2}$. To integrate this expression over a half-orbit is complicated by the fact that the two p factors appear with different time arguments. One requires an analytic expression for $p(t)$ in order to carry out this integral. It turns out that an excellent approximation

to $p(t)$ is obtained with just two Fourier components of the form

$$p(\varepsilon, t) \approx A(\varepsilon) \cos\left(\pi \frac{t}{t_\varepsilon}\right) + B(\varepsilon) \cos\left(3\pi \frac{t}{t_\varepsilon}\right). \quad (30)$$

We have explicitly indicated the energy dependence in p and in the coefficients. The latter are fixed by imposing two conditions. One is that the initial value of p be the correct one associated with its definition and the fact that $q(0) = 0$,

$$p(\varepsilon, 0) = A + B = \sqrt{2\varepsilon}. \quad (31)$$

The other is the equal-time average over a half orbit, already calculated for the Markovian case [cf. Eq. (27):

$$\frac{1}{t_\varepsilon} \int_0^{t_\varepsilon} p^2(t) dt = \frac{A^2 + B^2}{2} = \frac{4}{3t_\varepsilon}. \quad (32)$$

One obtains

$$\begin{aligned} A(\varepsilon) &= \sqrt{\frac{\varepsilon}{2}} + \sqrt{\frac{4}{3t_\varepsilon} - \frac{\varepsilon}{2}} \\ B(\varepsilon) &= \sqrt{\frac{\varepsilon}{2}} - \sqrt{\frac{4}{3t_\varepsilon} - \frac{\varepsilon}{2}}. \end{aligned} \quad (33)$$

Figure 6 is a typical example of the agreement between the exact deterministic $p(t)$ obtained via numerical integration and the approximation just presented. In this figure we have chosen an energy ε associated with our subsequent discussion of the transmission coefficient.

With this analytic expression for $p(t)$ one can now explicitly calculate the energy loss μ per half orbit. Substitution of Eq. (30) into Eq. (29), and integration over t between 0 and t_ε with fixed ε immediately leads to the expression

$$\frac{\mu}{\gamma} = \frac{t_\varepsilon}{2} \left(\frac{A^2}{1 + \left(\frac{\pi\tau}{t_\varepsilon}\right)^2} + \frac{B^2}{1 + \left(\frac{3\pi\tau}{t_\varepsilon}\right)^2} \right) - \tau \left(1 + e^{-t_\varepsilon/\tau} \right) \left(\frac{A}{1 + \left(\frac{\pi\tau}{t_\varepsilon}\right)^2} + \frac{B}{1 + \left(\frac{3\pi\tau}{t_\varepsilon}\right)^2} \right)^2 \quad (34)$$

with A and B given earlier. This result is shown in Fig. 7 for $\tau = 3.0$ and $\gamma = 0.01$.

The differences in Figs. 4 and 7 warrant discussion because of the “opposite” behaviors of

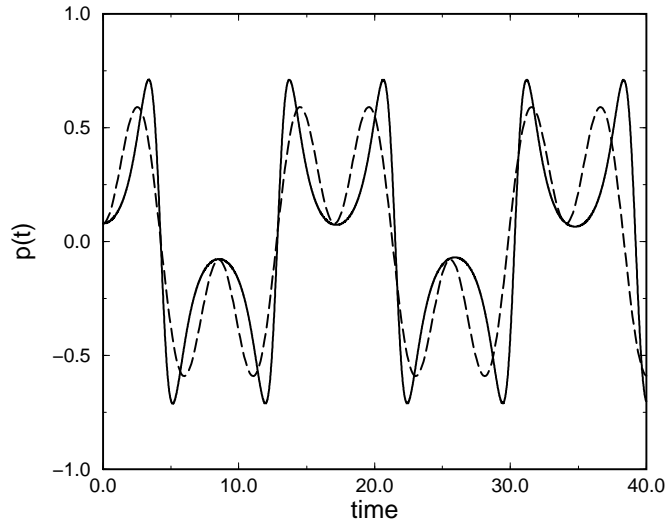


Figure 6: Momentum as a function of time for a particle moving in the potential (3) with energy $\varepsilon = 0.003175$ above the barrier. Solid curve: exact result. Dashed curve: approximation (30) with (33).

the energy loss per half orbit with increasing energy seen in the two figures. In the Markovian case ($\tau = 0$), the energy loss increases with increasing ε . Two opposing effects contribute to this behavior. On the one hand, the rate of energy loss is directly proportional to the kinetic energy of the particle and, on average, the kinetic energy increases with increasing ε . On the other hand, the energy loss in a half orbit increases with the time spent in this half orbit, and this time, t_ε , decreases with increasing ε . These competing effects more or less (but not entirely) compensate in the Markovian limit, and the result is a mild increase of μ with increasing ε . The situation becomes more complicated in the non-Markovian case, that is, when $\tau > 0$. Now the overwhelming factor in the ε dependence of the energy loss per half orbit is the relation between τ and t_ε . More specifically, it is the relation between $\pi\tau$ and t_ε , as seen from Eq. (34). In the regime $\pi\tau \ll t_\varepsilon$ one observes a behavior similar to the Markovian case, that is, in this regime μ increases with ε (in Eq. (34) this has been approximated by the upper bound discussed earlier, that is, by the constant $4\gamma/3$; in any case, this regime is not visible in Fig. 7). However, when $\pi\tau > t_\varepsilon$ the memory term is not fully dissipative (cf. discussion surrounding Eq. (17)) and hence leads to a smaller energy loss per half orbit. Since t_ε decreases with increasing ε , μ correspondingly decreases as well. Thus, for finite τ the energy loss per half orbit as a function of energy above the barrier is expected to exhibit

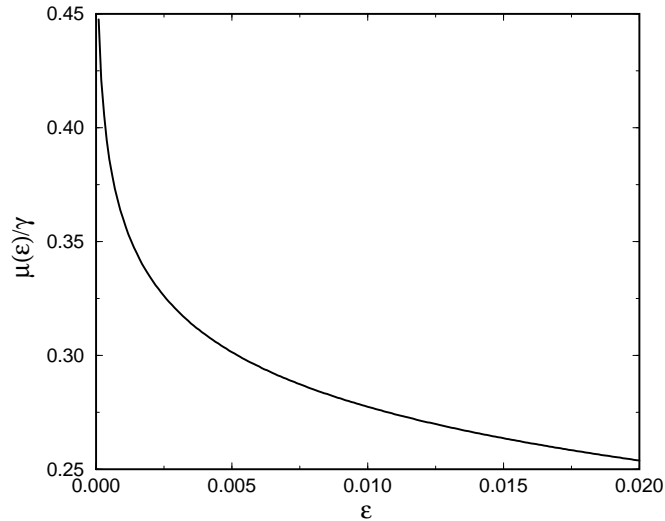


Figure 7: Energy loss per half orbit as a function of energy in the non-Markovian regime for correlation time $\tau = 3.0$ and dissipation parameter $\gamma = 0.01$.

a maximum. The behavior seen in Fig. 7 is that of μ to the right of this maximum. Note that τ would have to be extremely small in order to see the initial rise in μ (which in this approximation would be a flat region). Note also that although *both* Fourier components are needed to reproduce the behavior of $p(t)$, the behavior of $\mu(\varepsilon)$ is determined overwhelmingly by the principal (the first) Fourier component in Eq. (30).

From the result Eq. (34) we now wish to extract a specific (constant) value of μ to use in the calculation of the transmission coefficient. This is more difficult in the non-Markovian case than in the Markovian case because the variation of μ with ε is much more pronounced. However, one should remember that at low temperatures the population above the barrier is small and the principal contributors to the transmission coefficient are the particles near the barrier. Indeed, in the Markovian case we see from Fig. 5 that there are about five or six oscillations before the transmission coefficient settles down, indicating the participation of particles in a layer of width 5μ or so above the barrier. The variation of μ over a comparable range in Fig. 7 is actually rather small, that is, only a small portion of the range shown in the figure is actually important for the transmission coefficient. Thus, for instance, for $\tau = 3$ we find that the value of μ for those particles that half-orbit once before becoming trapped (found from Eq. (34) by setting $\varepsilon = \mu$ and solving for μ) is $\mu/\gamma = 0.3175$. For $\gamma = 0.01$ this corresponds to $\mu = 0.003175$. The variation of μ between

$\varepsilon = 0.003175$ and, say, five times this value, is about 15%. Thus, if we take $\mu = 0.003175$ we might overestimate μ by an amount only somewhat greater than that of the Markovian calculation, and expect the result to be comparably satisfactory.

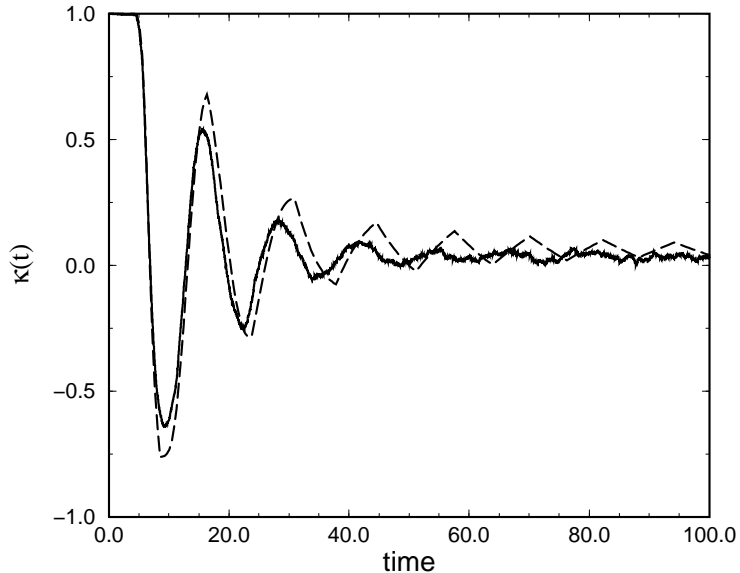


Figure 8: Transmission coefficient of an ensemble of particles at temperature $k_B T = 0.025$, dissipation parameter $\gamma = 0.01$, and dissipative memory time $\tau = 3.0$. Solid curve: simulation of 4000 particles. Dashed curve: our theory, Eq. (23) with $\mu = 0.003175$.

In Fig. 8 we show the simulation results as well as our theoretical result for a typical set of parameters. The simulation curve is one of those shown in Fig. 2. As in the Markovian case, the theory captures the distinctive features mentioned in the Markovian case: the time of the first abrupt drop of the transmission coefficient, the frequencies and amplitudes of the oscillations, and the asymptotic value. The theoretical overestimation of μ in the later oscillations is discernible (as it is in Fig. 5), and the calculated equilibrium transmission coefficient is also perhaps a bit high (as it is in Fig. 5). However, we understand the causes of these small effects and know how to correct the theory for them if needed. Also, the thermal corrections would bring the equilibrium transmission coefficient into even closer agreement with the simulation results, as in the Markovian case. Altogether, the theory is clearly very good in its prediction of the complex time-dependent and equilibrium behavior of the transmission coefficient in the non-Markovian regime for the case of an exponential memory kernel.

4 Conclusions

In this paper we have analyzed the time-dependent transmission coefficient for the generalized Kramers problem, that is, for a particle in a bistable potential described by a generalized Langevin equation. The transmission coefficient is associated with the rate of transitions of the particle from one well to the other. In this presentation the dissipative memory kernel has been taken to be exponential in time. In the diffusion-limited regime we have confirmed the predictions of Kohen and Tannor [6] via numerical simulations, and have shown their predictions to be accurate both in the non-adiabatic regime and in the caging regime. In the energy-diffusion-limited regime we have generalized our previous theory for the Markovian limit [10] to the non-Markovian case and have shown good agreement with numerical simulations in this regime as well. One can therefore say that there is now a fairly complete understanding of the time-dependent transmission coefficient for the generalized Kramers problem with an exponential memory kernel in the limiting regimes of strong dissipation and weak dissipation.

These remarks cover three of the four regimes represented by the simulations in Fig. 2, that is, the $\gamma = 2.0$, $\gamma = 10$, and $\gamma = 0.01$ curves. The fourth curve, the one for $\gamma = 0.3$, displays a distinct behavior that has not been discussed in this paper but that will be discussed elsewhere [20]. This represents an “intermediate” dissipation and is thus associated with a regime in which elements appropriate to the diffusion-limited regime and also to the energy-diffusion-limited regime in combination play an important role.

If one were to apply (misadvisedly) the KT theory to the left of the turnover in Fig. 1, one would find an apparent settling of the transmission coefficient at the values that in reality represent only the short-time plateau of $\kappa(t)$ seen in Fig. 2 before the first abrupt drop. Thus, for $\gamma = 0.01$ the transmission coefficient would settle at nearly unity and for $\gamma = 0.3$ it would settle at around 0.96. The actual abrupt drops seen in Fig. 2 following these initial plateaus come about because of the particles that have not been trapped after one half orbit and that at times t_ε cross the barrier to move over the left well. The diffusion-limited theory of course does not capture this recrossing and hence levels off. This leveling off has been referred to as an example of a “false plateau” that one must be careful of in interpreting simulation data. Perhaps more interesting “false plateau” manifestations occur as a result of memory kernels that are not exponential and that can lead to bottlenecks of various kinds in the relaxation process [19]. In general, one expects that different memory kernels might lead to behaviors not seen in the particular exponential model considered in

this paper. Our analysis of other memory kernels and the resultant exploration of interesting new dynamical manifestations of these differences will also be presented elsewhere [20].

Acknowledgment

This work was done during a sabbatical leave of J.M.S. at the University of California, San Diego granted by the Direcció General de Recerca de la Generalitat de Catalunya (Gaspar de Portolá program). The work was supported in part by the U.S. Department of Energy under Grant No. DE-FG03-86ER13606, and in part by the Comisión Interministerial de Ciencia y Tecnología (Spain) Project No. DGICYT PB96-0241.

References

- [1] H.A. Kramers, *Physica* **7** (1940) 284.
- [2] P. Hanggi, P. Talkner and M. Borkovec, *Rev. Mod. Phys.* **62** (1990) 251.
- [3] V. I. Melnikov, *Phys. Report* **209** (1991) 1.
- [4] E. Pollak, in *Activated Barrier Crossing*, eds. P. Hanggi and G. Fleming (World Scientific, Singapore, 1992).
- [5] S. C. Tucker, in *New Trends in Kramers Reaction Rate Theory: Understanding Chemical Reactivity*, eds. P. Talkner and P. Hanggi (Kluwer Academic, Dordrecht, 1995).
- [6] D. Kohen and D.J. Tannor, *J Chem. Phys.* **103** (1995) 6013.
- [7] R. F. Grote and J. T. Hynes, *J. Chem. Phys.* **73** (1980) 2715.
- [8] J. E. Straub and B.J. Berne, *J. Chem. Phys.* **83** (1985) 1138.
- [9] J. E. Straub, D.A. Hsu, and B.J. Berne, *J. Phys. Chem.* **89** (1985) 5188.
- [10] J. M. Sancho, A. H. Romero and K. Lindenberg, "The Kramers Problem in the Energy-Diffusion-Limited Regime," submitted for publication; cond-mat/9806001 (1998).
- [11] J. E. Straub and B. J. Berne, *J. Chem. Phys.* **85** (1986) 2999.
- [12] R. Zwanzig, *J. Chem. Phys.* **86** (1987) 5801.

- [13] T.C. Gard, *Introduction to Stochastic Differential Equations*, Marcel Dekker, vol.114 of *Monographs and Textbooks in Pure and Applied Mathematics* (1987).
- [14] R. Toral, in *Computational Field Theory and Pattern Formation*, 3rd Granada Lectures in Computational Physics, Lecture Notes in Physics Vol. 448 (Springer Verlag, Berlin, 1995).
- [15] S. Adelman, *J. Chem. Phys.* **64** (1976) 124.
- [16] R. L. Stratonovich, *Topics in the Theory of Random Noise*, Vol. 1 (1963) and Vol. 2 (1967) (Gordon and Breach, New York).
- [17] K. Lindenberg and B. J. West, *The Nonequilibrium Statistical Mechanics of Open and Closed Systems* (VCH, New York, 1990).
- [18] V. I. Melnikov, *Phys. Rev. E* **48** (1993) 3271.
- [19] S. Tucker, *J. Chem. Phys.* **101** (1994) 2006; S. K. Reese, S. Tucker, and G. K. Schenter, *J. Chem. Phys.* **102** (1995) 104.
- [20] R. Reigada, A. H. Romero, J. M. Sancho, and K. Lindenberg, in preparation.

Figure 1: Transmission coefficient κ_{st} vs dissipation parameter γ for $k_B T = 0.025$ and various values of the memory correlation time τ . These results are obtained from direct simulation of Eq. (1) as described in Section 2.2. As is well known, the turnover moves to higher values of the friction parameter with increasing τ because the effective dissipation at given γ is weaker as τ increases. Also, the maximum transmission coefficient decreases with increasing τ .

Figure 2: Numerical simulation results for the transmission coefficient $\kappa(t)$ vs time for memory correlation time $\tau = 3.0$ and temperature $k_B T = 0.025$, and four values of the dissipation parameter γ . Diffusion-limited non-adiabatic regime: $\gamma = 2$; diffusion-limited caging regime: $\gamma = 10$; energy-diffusion-limited regime: $\gamma = 0.01$; intermediate regime: $\gamma = 0.3$.

Figure 3: Numerical simulation results and theoretical results for the transmission coefficient $\kappa(t)$ vs time for memory correlation time $\tau = 3.0$ and temperature $k_B T = 0.025$, and two values of the dissipation parameter γ in the diffusion-limited regime. Solid curves: simulation results for $\gamma = 2.0$ (diffusion-limited non-adiabatic regime) and $\gamma = 10.0$ (diffusion-limited caging regime). The dashed curves in each case are calculated from the theory of Kohen and Tannor as given in Eq. (13).

Figure 4: Energy loss per half orbit as a function of energy in the Markovian limit ($\tau \rightarrow 0$) for two values of the dissipation parameter: $\gamma = 0.005$ (dashed curve) and $\gamma = 0.01$ (solid curve).

Figure 5: Transmission coefficient of an ensemble of particles at temperature $k_B T = 0.025$ and dissipation parameter $\gamma = 0.005$ in the Markovian limit. Solid curve: simulation of 4000 particles. Dashed curve: our theory, Eq. (23), with the bare value $\mu = 4\gamma/3 = 0.006667$. Thick line that intersects the right vertical axis: value of the equilibrium transmission coefficient κ_{st} obtained from Eq. (26) using the value of μ renormalized by thermal fluctuations, which for this temperature is $\mu(T) = 0.004907$.

Figure 6: Momentum as a function of time for a particle moving in the potential (3) with energy $\varepsilon = 0.003175$ above the barrier. Solid curve: exact result. Dashed curve: approximation (30) with (33).

Figure 7: Energy loss per half orbit as a function of energy in the Markovian limit ($\tau \rightarrow 0$) for two values of the dissipation parameter: $\gamma = 0.005$ (dashed curve) and $\gamma = 0.01$ (solid curve).

Figure 8: Transmission coefficient of an ensemble of particles at temperature $k_B T = 0.025$, dissipation parameter $\gamma = 0.01$, and dissipative memory time $\tau = 3.0$. Solid curve: simulation of 4000 particles. Dashed curve: our theory, Eq. (23) with $\mu = 0.003175$.